SOX2 regulates paclitaxel resistance of A549 non-small cell lung cancer cells via promoting transcription of ClC-3

YOUWEI HUANG[1*], XIANGYU WANG[1*], RENDONG HU[1,2*], GUOPENG PAN[1] and XI LIN[1]

[1]Department of Pharmacology, School of Medicine, Jinan University, Guangzhou, Guangdong 510632; [2]School of Medicine, South China University of Technology, Guangzhou, Guangdong 510006, P.R. China

Received May 30, 2022; Accepted August 17, 2022

DOI: 10.3892/or.2022.8396

Abstract. Paclitaxel (PTX) is widely used in the treatment of non-small cell lung cancer (NSCLC). However, acquired PTX drug resistance is a major obstacle to its therapeutic efficacy and the underlying mechanisms are still unclear. The present study revealed a novel role of the SRY-box transcription factor 2 (SOX2)-chloride voltage-gated channel-3 (ClC-3) axis in PTX resistance of A549 NSCLC cells. The expression levels of SOX2 and ClC-3 were upregulated in PTX-resistant A549 NSCLC cells by RT-qPCR and western blotting. The drug resistance to PTX of A549 NSCLC cells were measured by detecting the cell viability and the expression of drug resistance markers. Knockdown of SOX2 or ClC-3 effectively decreased PTX resistance of A549 NSCLC cells, whereas SOX2 or ClC-3 overexpression promoted PTX resistance. Mechanistically, SOX2 bound to the promoter of ClC-3 and enhanced the transcriptional activation of ClC-3 expression by CUT&Tag assays, CUT&Tag qPCR and luciferase reporter. In summary, the present findings defined ClC-3 as an important downstream effector of SOX2 and ClC-3 and SOX2 contributed to PTX resistance. Targeting SOX2 and its downstream effector ClC-3 increased the sensitivity of NSCLC cells to PTX treatment, which provided potential therapeutic strategies for patients with NSCLC with PTX resistance.

Introduction

Lung cancer is the leading cause of cancer mortality among men and women worldwide and causes 1.59 million deaths each year (1,2). Histopathologically, lung cancer is divided into non-small cell lung cancer (NSCLC) and small-cell lung cancer and is usually diagnosed at a late stage because it often has no symptoms until it has spread (3). Furthermore, ~85% of lung cancers are NSCLC, of which >50% are advanced at the time of diagnosis and the 5-year survival rate for all stages of NSCLC is <15% (4,5). In the late stage, the most common symptoms include cough, dyspnea and hemoptysis and the cancer has metastasized beyond the lungs and into other areas of the body, such as the lymph nodes, brain or other organs (6). At present, surgery and paclitaxel (PTX)- or platinum-based combination chemotherapy are the most common applications in the clinical treatment of NSCLC (7). PTX is a tubulin-disrupting agent and has demonstrated antitumor efficacy against a broad variety of tumors, such as lung, breast and ovarian cancer (8,9). PTX is a first-line chemotherapy drug in the treatment of advanced NSCLC (10). The initial response to PTX in the treatment of NSCLC is favorable; however, the patients often develop drug resistance to PTX leading to treatment failure (11). Therefore, it is urgent to investigate the mechanism underlying the development of PTX resistance and to develop novel therapeutic strategies for overcoming PTX resistance.

The chloride voltage-gated channel-3 (ClC-3) is a member of the ClC voltage-gated Cl^- channel family. Accumulating studies have suggested that ClC-3 is expressed in a number of cancer cells and serves a well-defined role in cell proliferation, apoptosis and metastasis (12-15). Furthermore, abnormality of ClC-3 expression has been demonstrated to be associated with the development of drug resistance, including PTX, cisplatin and etoposide resistance, in various tumor cells (16-19). However, the potential regulatory mechanism of ClC-3 in PTX resistance of NSCLC remains largely unknown.

Cancer stem cells (CSCs) are a small subpopulation of cancer cells with characteristics that are associated with stem cells (20). CSCs are considered to be the main cause of chemotherapy resistance (21,22). SRY-box transcription factor 2 (SOX2) is not only a pluripotent stem cell-related factor but also a key transcription factor and serves a role in maintaining stem cell properties and determining the fate of cells (23). Researchers have revealed that SOX2 is aberrantly expressed in different types of cancer and that SOX2 expression is positively associated with cancer cell stemness and multi-drug resistance (24-26). Therefore, SOX2 may be an attractive therapeutic target for overcoming chemotherapy resistance.

Correspondence to: Professor Xi Lin, Department of Pharmacology, School of Medicine, Jinan University, 601 West Huangpu Avenue, Guangzhou, Guangdong 510632, P.R. China
E-mail: linx_jnu@163.com

*Contributed equally

Key words: SRY-box transcription factor 2, chloride voltage-gated channel 3, non-small-cell lung cancer, paclitaxel resistant, stemness, transcription

In the present study, SOX2 and ClC-3 were highly expressed in PTX-resistant A549 NSCLC cells and SOX2 increased the sensitivity of A549 NSCLC cells to PTX treatment via downregulation of the levels of ClC-3. The molecular mechanism between SOX2 and ClC-3 was further explored using cleavage under targets and tagmentation (CUT&Tag) sequencing prediction results. Taken together, the present study provided novel insights into targeting the SOX2/ClC-3 axis as a potential therapeutic strategy for patients with NSCLC with PTX resistance.

Materials and methods

Cell lines and cell culture. Human A549 NSCLC cell lines were obtained from American Type Culture Collection. The PTX-resistant A549 NSCLC (A549-PTX) cells were established by gradual exposure of A549 cells to increasing concentrations of PTX, as previously described (27). In order to maintain the PTX-resistant phenotype of A549-PTX cells, 0.1 μM PTX was added into the culture medium. The A549 cells used in the present study were cultured in parallel during the establishment of A549-PTX cells. All cells were cultured in DMEM (Corning, Inc.) supplemented with 10% fetal bovine serum (Gibco; Thermo Fisher Scientific, Inc.) and 1X penicillin/streptomycin (HyClone; Cytiva). All cultures were maintained in a humidified tissue culture incubator at 37˚C with 5% CO_2.

Cell transfection. For RNA interference, SOX2 small interfering RNA (siRNA/si) and ClC-3 siRNA were purchased from Guangzhou RiboBio Co., Ltd. $2x10^5$ cells per well were seeded in 6-well plates for 24 h before transfection. Subsequently, cells were transfected with SOX2 siRNA (25 nM), ClC-3 siRNA (25 nM) or their negative control (siNC, (25 nM)) using Lipofectamine® RNAiMAX Transfection Reagent (Invitrogen; Thermo Fisher Scientific, Inc.) according to the manufacturer's instructions. Following transfection for 12 h in a humidified tissue culture incubator at 37˚C with 5% CO_2, the fresh medium with 10% FBS was replaced and incubated for 48 h. The siRNA target sequences used are presented in Table I.

Lentiviral infection. Human SOX2 and ClC-3 were subcloned into the lentiviral plasmids pCMV-3XFlag-Puro vector and the plasmids and lentivirus particles were generated by OBiO Technology (Shanghai) Corp., Ltd. Lentivirus were produced in 293T cells using a third generation lentiviral system (Shanghai OBiO Technology Co., Ltd.). Briefly, $5x10^6$ 293T cells were seeded in a 100-mm culture dish at 24 h before transfection. 5 μg lentiviral construct and 5 μg lentiviral envelope and packaging plasmids (both from Shanghai OBiO Technology Co., Ltd.) were co-transfected into 293T cells (the mixed ratio was lentiviral construct: lentiviral envelope and packaging plasmids, 1:1) by using Lentiviral Packaging Transfection kit (Shanghai OBiO Technology Co., Ltd.). Following transfection for 8 h at 37˚C in a CO_2 incubator, the medium was replaced with fresh culture medium. After 48 h, the lentivirus-containing supernatants were harvested, centrifuged at 2,000 x g for 10 min at room temperature and filtered by using 0.22 μm filter. The cells were infected with the 10 MOI lentivirus of empty vector pCMV-3XFlag-Puro, pCMV-ClC-3-3Xflag-Puro or pCMV-SOX2-3Xflag-Puro construct to create SOX2- or ClC-3-overexpressing stable cell lines. Cells were infected with 10 MOI lentivirus and then selected in medium containing 1 μg/ml puromycin for 1 week. Finally, cells were maintained in medium containing 0.1 μg/ml puromycin medium. SOX2 or ClC-3 expression was confirmed by western blot analysis.

Cell counting kit-8 (CCK-8) assays. Cell viability was evaluated using CCK-8 (Dojindo Molecular Technologies, Inc.) according to the manufacturer's protocol. Briefly, 5,000 cells per well were seeded in 96-well plates and allowed to adhere overnight. Cells were then treated with different concentrations of PTX or DIDS for 48 h. Next, DMEM containing 10% CCK-8 solution was supplemented into each well and the cells were incubated in a 37˚C incubator for 2 h. The optical density of each well was measured using a microplate reader (Synergy H1; BioTeke Corporation) at a wavelength of 450 nm. The cytotoxicity of PTX to cell lines was evaluated.

Cell colony formation assays. A total of $1x10^3$ cells per well were seeded in 6-well plates and incubated for 24 h, following treatment with PTX (50 or 100 μM) or DMSO as a control in a humidified tissue culture incubator at 37˚C with 5% CO_2 for 48 h. Media were replaced every 3 days. After 2 weeks of growth, the medium was discarded and the cells were fixed with 4% formaldehyde, following Please give temperature and duration of staining. according to the manufacturer's instructions. Images were captured using a digital scanner (Canon, Inc.). Colonies were counted using ImageJ 1.80 software (National Institutes of Health).

Reverse transcription-quantitative PCR (RT-qPCR). Total RNA was extracted from cultured cells at 80% confluence using TRIzol® (Thermo Fisher Scientific, Inc.) according to the manufacturer's protocol. cDNA synthesis was carried out using SuperScript II Reverse Transcriptase and random hexanucleotide primers (Invitrogen; Thermo Fisher Scientific, Inc.) according to the manufacturer's protocols. qPCR was performed using synthesized primers (Tsingke Biological Technology) and SYBR green master mix (Tiangen Biotech Co., Ltd.) to detect the mRNA levels. PCR conditions were as follows: Pre-denaturation at 95˚C for 1 min; followed by 40 cycles of denaturation at 95˚C for 20 sec, annealing at 60˚C for 20 sec and elongation at 72˚C for 30 sec. The reaction was performed using an Applied Biosystems 7500 Fast Sequence Detection system (Applied Biosystems; Thermo Fisher Scientific, Inc.). The expression levels of the target genes were quantitated using the $2^{-\Delta\Delta Cq}$ method and β actin (*ACTB*) was used as the internal control to normalize the qPCR data (28). The primer sequences are presented in Table II. All samples were examined at least three times.

Western blotting and immunoprecipitation (IP) assays. Protein was extracted from cells using M-PER (Thermo Fisher Scientific, Inc.) and the protein concentration was determined using a BCA Protein Assay Kit (Thermo Fisher Scientific, Inc.). The protein extracts (20 μg per lane) were separated by using 10% SDS-PAGE and then transferred to a

Table I. siRNA target sequences.

siRNA	Target sequences (5'-3')
siClC-3-1	CCTGGTTCTTATATCATGA
siClC-3-2	GATGGCTAGTAGTAACACT
siClC-3-3	GCCTTAGTGCGTTGTGGTA
siSOX2-1	CCAAGACGCTCATGAAGAA
siSOX2-2	GGAGCACCCGGATTATAAA
siSOX2-3	GCTCGCAGACCTACATGAA

siRNA/si, small interfering RNA; ClC-3, chloride voltage-gated channel 3.

polyvinylidene fluoride (PVDF) membrane (MilliporeSigma), followed by blocking with 5% skimmed milk powder in room temperature for 1 h and incubation with primary antibodies overnight at 4˚C. The primary antibodies used were: ClC-3 (1:1,000; cat. no. 13359; Cell Signaling Technology, Inc.), SOX2 (1:1,000; cat. no. 23064; Cell Signaling Technology, Inc.), octamer-binding transcription factor 4 (OCT4; 1:1,000; cat. no. 2750; Cell Signaling Technology, Inc.), NANOG (1:1,000; cat. no. 4903; Cell Signaling Technology, Inc.), KLF transcription factor 4 (KLF4; 1:1,000; cat. no. 4038; Cell Signaling Technology, Inc.), multidrug resistance mutation 1 (MDR1; 1:1,000; cat. no. 13342; Cell Signaling Technology, Inc.), ATP binding cassette subfamily C member 2 (ABCC2; 1:1,000; cat. no. 4446; Cell Signaling Technology, Inc.), ATP binding cassette subfamily C member 10 (ABCC10; 1:1,000; cat. no. ab69296; Abcam), GAPDH (1:10,000; cat. no. ARG65680; Arigo Biolaboratories Corp.) and tubulin (1:10,000; cat. no. ARG65693; Arigo Biolaboratories Corp.). Subsequently, the membranes were incubated with peroxidase-conjugated secondary antibody. The secondary antibodies used were Goat anti-Rabbit IgG (1:10,000; cat. no. ARG65351; Arigo Biolaboratories Corp.) and Goat anti-Mouse IgG (1:10,000; cat. no. ARG65350; Arigo Biolaboratories Corp.). The protein signals were determined using the ChemiDoc XRS+ System (Bio-Rad Laboratories, Inc.) and the ECL detection kit (MilliporeSigma). The gray value of the protein bands was analyzed by ImageJ software (version: 1.53; National Institutes of Health).

For IP analysis, the cells were treated with 30 μM MG132 for 6 h in a tissue culture incubator at 37˚C with 5% CO_2 before collection and then the cells were lysed in IP lysis buffer (Beyotime Biotechnology Inc.). Next, the lysates were immunoprecipitated with antibody of SOX2 (1:100; cat. no. 23064; Cell Signaling Technology, Inc.) or ClC-3 (1:50; cat. no. 13359; Cell Signaling Technology, Inc.) together with Protein A/G magnetic beads at 4˚C overnight. The samples were boiled in 5X loading buffer for 10 min and then separated from the beads using magnetic separator. The samples were detected by western blot analysis according to the aforementioned procedure.

CUT&Tag assays and CUT&Tag qPCR. The CUT&Tag assay was performed using a NovoNGS CUT&Tag 3.0 HighSensitivity kit (Novoprotein Scientific Inc.) according to the manufacturer's instructions. Briefly, NovoNGS ConA Beads were washed using ConA Binding Buffer. A total of $1x10^5$ A549 cells were harvested and washed using 1X wash buffer. The cells with beads were incubated with the SOX2 antibody (1:50; cat. no. 23064; Cell Signaling Technology, Inc.) overnight at 4˚C, followed by incubation with a secondary antibody at room temperature for 1 h. The secondary antibody used was Goat anti-Rabbit IgG H&L (1:100, cat. no. N269-01A; Novoprotein Scientific Inc.). After washing away the unbounded secondary antibody, the cells were incubated with NovoNGS ChiTag pA-Tn5 for 1 h at room temperature. Next, the cells were washed by ChiTag Buffer, followed by tagmentation using Tagmentation Buffer for 1 h at 37˚C. The tagmentation reaction was stopped by addition of 10% SDS at 55˚C for 10 min. DNA was isolated using Tagment DNA Extract Beads (Novoprotein Scientific Inc.) and dissolved in TE Buffer. DNA was amplified with N5 and N7 primers and purified with NovoNGS DNA Clean Beads for sequencing and qPCR assays. For CUT&Tag sequencing, the libraries were sequenced and analyzed by Guangzhou Epibiotek Co., Ltd. Briefly, the reads were aligned using Bowtie2 (version: 2.2.9; http://bowtie-bio.sourceforge.net/bowtie2/index.shtml). Peak calling was performed with MACS2 (version: 2.1.1; https://pypi.org/project/MACS2/2.1.1.20160309/) and annotated using HOMER (http://homer.ucsd.edu/homer/). The heatmap was generated using deepTools (version: 2.4.1; http://deeptools.ie-freiburg.mpg.de/). The peaks visualization in the genome was shown by IGV software (version: 2.13.2; http://software.broadinstitute.org/software/igv). Functional Gene Ontology (GO) enrichment analysis were performed using GENEONTOLOGY database (http://geneontology.org/). The purified DNA from the CUT&Tag assay was quantified by qPCR using SuperReal PreMix SYBR Green on an Applied Biosystems 7500 Fast Sequence Detection system. The ClC-3 binding sites of SOX2 at the gene promoter regions were predicted in CUT&Tag sequencing and primers were designed by Primer software. The primers of the *CLCN3* promoter used were as follows: Forward, 5'-AACCTCCGCCTTCCA-3'; Reverse, 5'-AAACCAGCCTGAGCAAC-3'.

Luciferase reporter assays. The luciferase reporter plasmid containing the putative ClC-3 promoter in pGL4 basic vector were purchased by OBiO Technology Corp., Ltd. Luciferase reporter assays were carried out in A549-ClC-3 and empty vector stably transfected cells. Cells were transfected with ClC-3 promoter and *Renilla* luciferase plasmids in 6-well plates using Lipofectamine® 3000 according to the manufacturer's instructions (Invitrogen; Thermo Fisher Scientific, Inc.). After 48 h of transfection, the luciferase activity was measured using the Dual-Luciferase Reporter Assay System (Promega Corporation) according to the manufacturer's instructions and the cell lysates were analyzed by western blot analysis according to the aforementioned procedure.

Graphic scheme of study methodology. The stages of study methodologies are shown in Fig. S1.

Statistical analysis. All statistical analyses were performed using GraphPad Prism (8.0; GraphPad Software, Inc.) and all data were repeated at least three times from three independent

Table II. Primer sequences.

Gene	Forward primer (5'-3')	Reverse primer (5'-3')
CLCN3	CCTCTTTCCAAAGTATAGCAC	TTACTGGCATTCATGTCATTTC
SOX2	TACAGCATGTCCTACTCGCAG	GAGGAAGAGGTAACCACAGGG
OCT4	GCAGCGACTATGCACAACGA	CCAGAGTGGTGACGGAGACA
KLF4	ATCTTTCTCCACGTTCGCGTCTG	AAGCACTGGGGGAAGTCGCTTC
Nanog	AAGGTCCCGGTCAAGAAACAG	CTTCTGCGTCACACCATTGC
P-gp	GCTGTCAAGGAAGCCAATGCCT	TGCAATGGCGATCCTCTGCTTC
MDR1	CCCATCATTGCAATAGCAGG	TGTTCAAACTTCTGCTCCTGA
ABCC2	GCCAACTTGTGGCTGTGATAGG	ATCCAGGACTGCTGTGGGACAT
ABCC10	CCTAGTGCTGACCGTGTTGT	TAGGTTGGCTGCAGTCTGTG
ACTB	CACCATTGGCAATGAGCGGTTC	AGGTCTTTGCGGATGTCCACGT

CLCN3, chloride voltage-gated channel 3; SOX2, SRY-box transcription factor 2; *KLF4*, KLF transcription factor 4; *P-gp*, P-glycoprotein; *MDR1*, multidrug resistance mutation 1; *ABCC2*, ATP binding cassette subfamily C member 2; *ABCC10*, ATP binding cassette subfamily C member 10; *ACTB*, beta actin; *OCT4*, octamer-binding transcription factor 4.

experiments for analysis and are presented as the mean ± standard deviation. The normality of the data was tested by Shapiro-Wilk test and all of the datasets are homogeneity of variance. Unpaired two-tail Student's t-test was used to analyze the difference between the two groups (Figs. 1A-D, 2B, C and F, 3B, D, E and H). The difference between the three groups of data were analyzed by one-way ANOVA. Dunnett test was used for multiple comparisons of cell viability (Figs. 1E, 2E, 3G, 5B and D). Tukey's HSD test was used for multiple comparisons of protein expression (Figs. 4H and I, 5A and C). $P<0.05$ was considered to indicate a statistically significant difference.

Results

Establishment of PTX-resistant A549 NSCLC cells. A549 cells were cultured with 1 μM PTX for >6 months to establish the PTX-resistant A549 subline as described in a previous study (27). In order to verify whether the established A549 cells were resistant to PTX, the proliferation of A549-PTX cells and the parental A549 cells treated with PTX was compared in CCK-8 and colony formation assays. The results of the CCK-8 assay revealed that the viability of A549-PTX cells was higher compared with that of A549 cells (Fig. 1A). Additionally, the results of the colony formation assays indicated that the proliferation capacity was strongly increased in A549-PTX cells at the same concentration of PTX compared with A549 cells (Fig. 1B). Subsequently, the levels of drug resistance markers in A549 and A549-PTX cells were compared using RT-qPCR and western blotting. RT-qPCR and western blotting revealed increased expression levels of P-glycoprotein (P-gp), MDR1, ABCC2 and ABCC10 in A549-PTX cells (Fig. 1C and D). Overall, the data indicated that the establishment of PTX-resistant A549 cells was successful.

ClC-3 promotes PTX resistance in A549 NSCLC cells. It has been reported that ClC-3 contributes to PTX resistance in A549 NSCLC cells (17). ClC-3 was significantly upregulated in A549-PTX cells consistent with the results of previous studies (16,17). To verify the role of ClC-3 in PTX resistance, 4,4-diisothiocyanatostilbene-2,2-disulfonate (DIDS), a specific chloride channel inhibitor, was used. CCK-8 assays revealed that DIDS increased the sensitivity of A549-PTX cells to PTX (Fig. 1E). Subsequently, the present study examined whether ClC-3 directly modulated PTX resistance. The expression levels of ClC-3 in A549-PTX cells were knocked down by exogenous introduction of ClC-3 siRNAs (siClC-3-1, siClC-3-2 and siClC-3-3). Western blotting was conducted to detect the knockdown efficiency and the results demonstrated that transfection with siClC-3-3 led to a reduction of ClC-3 expression in A549-PTX cells and used in subsequent assays (Fig. 2A). CCK-8 assays revealed that ClC-3 silencing significantly increased the sensitivity of A549-PTX cells to PTX (Fig. 2B). Western blotting demonstrated that knockdown of ClC-3 downregulated the expression levels of MDR1, ABCC2 and ABCC10 in A549-PTX cells (Fig. 2C). Next, ClC-3 was overexpressed in A549 cells by infection with lentiviral vector and the overexpression efficiency of ClC-3 was verified by western blotting (Fig. 2D). The CCK-8 assay results revealed that ClC-3 overexpression decreased the sensitivity of A549 cells to PTX (Fig. 2E) and western blot analysis revealed that ClC-3 overexpression upregulated the expression levels of MDR1, ABCC2 and ABCC10 in A549 cells (Fig. 2F). Taken together, these results indicated that ClC-3 was upregulated in A549-PTX cells and that ClC-3 is required for sustaining PTX resistance in A549 NSCLC cells. Western blotting demonstrated that knockdown of ClC-3 downregulated the expression levels of MDR1, ABCC2 and ABCC10 in A549-PTX cells.

Higher levels of SOX2 confer PTX resistance in A549 NSCLC cells. Previous reports have demonstrated that stemness factors are involved in the development of multi-drug resistance (20,21,29). Initially, the expression levels of stemness factors were examined by RT-qPCR and it was observed that *SOX2*, *OCT4* and *NANOG* were downregulated and *KLF4* expression was not significantly altered in A549-PTX cells compared with A549 cells (Fig. 3A). The results of western

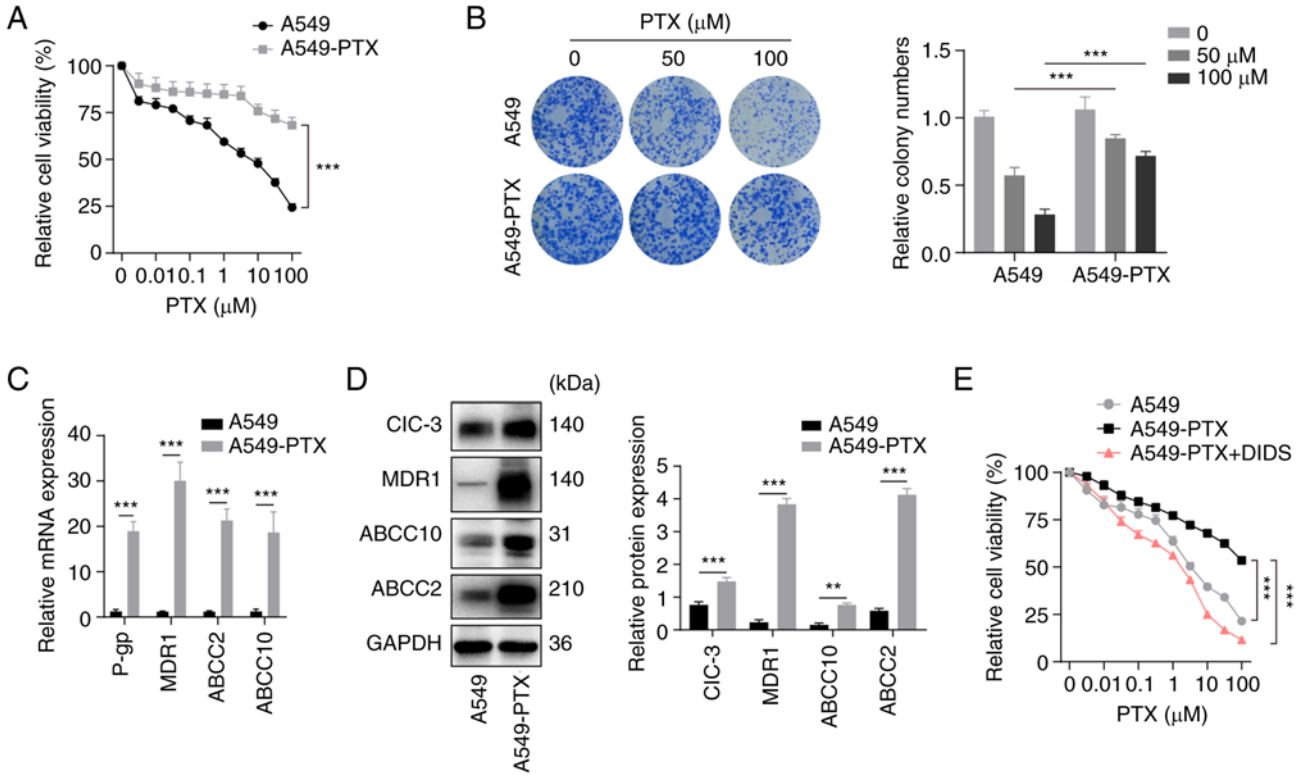

Figure 1. Establishment of PTX-resistant A549 non-small cell lung cancer cells. (A) Viability was assessed using CCK-8 assays in A549 and A549-PTX cells treated with PTX for 48 h. (B) (Left) Cell proliferation was examined by colony formation assays in A549 and A549-PTX cells treated with PTX. (Right) Colony numbers as quantified using ImageJ. (C) mRNA expression levels of drug resistance-related genes were measured by reverse transcription-quantitative PCR in A549 and A549-PTX cells. (D) (Left) Protein expression levels of ClC-3, MDR1, ABCC10, ABCC2 and GAPDH were examined by western blotting in A549 and A549-PTX cells. (Right) Protein expression was semi-quantified using ImageJ. (E) Viability was assessed using CCK-8 assays in A549, A549-PTX or DIDS-treated A549-PTX cells treated with PTX for 48 h. DIDS, 10 μM for 48 h. GAPDH was used as a loading control in western blotting. All data are presented as the mean ± standard deviation. **P<0.01, ***P<0.001. Relative, vs. respective control. PTX, paclitaxel; CCK-8, Cell Counting Kit-8; A549-PTX cells, PTX-resistant A549 NSCLC cells; CIC-3, chloride voltage-gated channel 3; MDR1, multidrug resistance mutation 1; ABCC10, ATP binding cassette subfamily C member 10; ABCC2, ATP binding cassette subfamily C member 2; DIDS, 4,4-diisothiocyanatostilbene-2,2-disulfonate.

blotting demonstrated that SOX2 was upregulated but OCT4, KLF4 and NANOG were downregulated in A549-PTX cells compared with A549 cells (Fig. 3B). The present study next examined whether SOX2 is required for PTX resistance in A549 NSCLC cells. The expression levels of SOX2 were knocked down in A549-PTX cells by exogenous introduction of SOX2 siRNAs (siSOX2-1, siSOX2-2 and siSOX2-3). Western blot analysis was conducted to detect the knockdown efficiency and the results indicated that siSOX2-1 led to a reduction of SOX2 expression in A549-PTX cells and used in subsequent assays (Fig. 3C). CCK-8 assays demonstrated that SOX2 silencing significantly increased the sensitivity of A549-PTX cells to PTX (Fig. 3D). Western blot analysis demonstrated that knockdown of SOX2 downregulated the expression levels of MDR1, ABCC2 and ABCC10 in A549-PTX cells (Fig. 3E). Next, SOX2 was overexpressed in A549 cells by infection with lentiviral vector and the overexpression efficiency of SOX2 was verified by western blotting (Fig. 3F). The CCK-8 assay results revealed that SOX2 overexpression decreased the sensitivity of A549 cells to PTX (Fig. 3G) and western blot analysis demonstrated that SOX2 overexpression upregulated the expression levels of MDR1, ABCC2 and ABCC10 in A549 cells (Fig. 3H). Taken together, the data suggested that SOX2 mediated the PTX resistance of NSCLC cells.

SOX2 promotes ClC-3 transcription. Our previous study revealed that SOX2 interacts with ClC-3 in DU145 prostatic carcinoma cells and contributes to tumorigenesis (30). To further examine whether there was a potential interaction between ClC-3 and SOX2 in PTX-resistant A549 NSCLC cells, the interaction of SOX2 and ClC-3 was detected using an IP assay. The IP assay demonstrated that there was no interaction between ClC-3 and SOX2 in A549 cells (Fig. 4A). To further examine the potential regulation between ClC-3 and SOX2, western blotting was performed and revealed that SOX2 expression was increased after transfection with siClC-3 in A549 cells and ClC-3 overexpression downregulated SOX2 expression in A549 cells (Fig. 4B). However, knockdown of SOX2 downregulated the levels of ClC-3 and SOX2 overexpression upregulated the expression levels of ClC-3 in A549 cells (Fig. 4C). These results revealed that ClC-3 is a downstream effector of SOX2. Given that SOX2 is a transcription factor (31), the present study demonstrated that SOX2 could bind to the promoter region of ClC-3 and examined the binding sites using CUT&Tag in A549 cells. CUT&Tag using antibodies against SOX2 and analysis with deepTools revealed clear enrichment of SOX2 peaks and SOX2 peaks were localized in the transcription start site of gene promoters (±3 kb) in A549 cells (Fig. 4D). The wide genomic distribution of SOX2 in A549 cells is shown in Fig. 4E. Next, to investigate

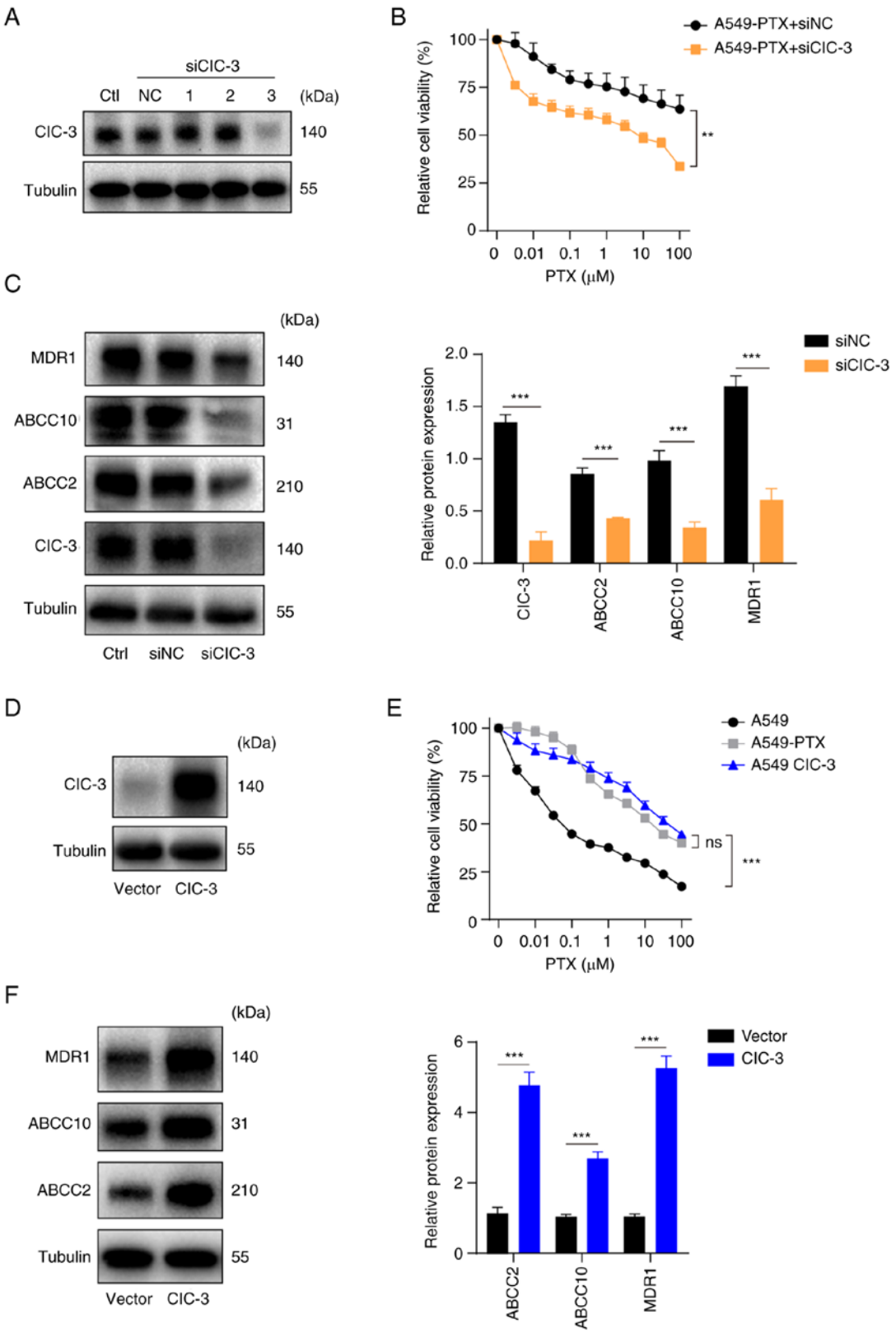

Figure 2. ClC-3 is upregulated in PTX-resistant A549 cells. (A) ClC-3 protein expression was measured by western blotting in A549-PTX cells transfected with siNC or ClC-3 siRNA (siClC-3-1, siClC-3-2 and siClC-3-3). (B) Viability was examined by CCK-8 assays in A549-PTX cells transfected with siClC-3 or control treated with PTX for 48 h. (C) (Left) Protein expression levels of MDR1, ABCC10, ABCC2 and ClC-3 were examined by western blotting in A549-PTX cells transfected with siClC-3 or control. (Right) Protein expression was semi-quantified using ImageJ. (D) Protein expression levels of ClC-3 were examined by western blotting in A549 cells overexpressing ClC-3 or its vector control. (E) Viability was examined by CCK-8 assays in A549, A549-PTX and ClC-3-overexpressing A549 cells treated with PTX for 48 h. (F) (Left) Protein expression levels of MDR1, ABCC10 and ABCC2 were examined by western blotting in A549 cells overexpressing ClC-3 or its vector control. (Right) Protein expression was semi-quantified using ImageJ. Tubulin was used as a loading control in western blotting. All data are presented as the mean ± standard deviation. **P<0.01, ***P<0.001. ns, not significant. Relative, vs. respective control. ClC-3, chloride voltage-gated channel 3; PTX, paclitaxel; A549-PTX cells, PTX-resistant A549 non-small cell lung cancer cells; siRNA/si, small interfering RNA; siNC, control siRNA; ClC-3, chloride voltage-gated channel 3; MDR1, multidrug resistance mutation 1; ABCC10, ATP binding cassette subfamily C member 10; ABCC2, ATP binding cassette subfamily C member 2; CCK-8, Cell Counting Kit-8; Ctl, control.

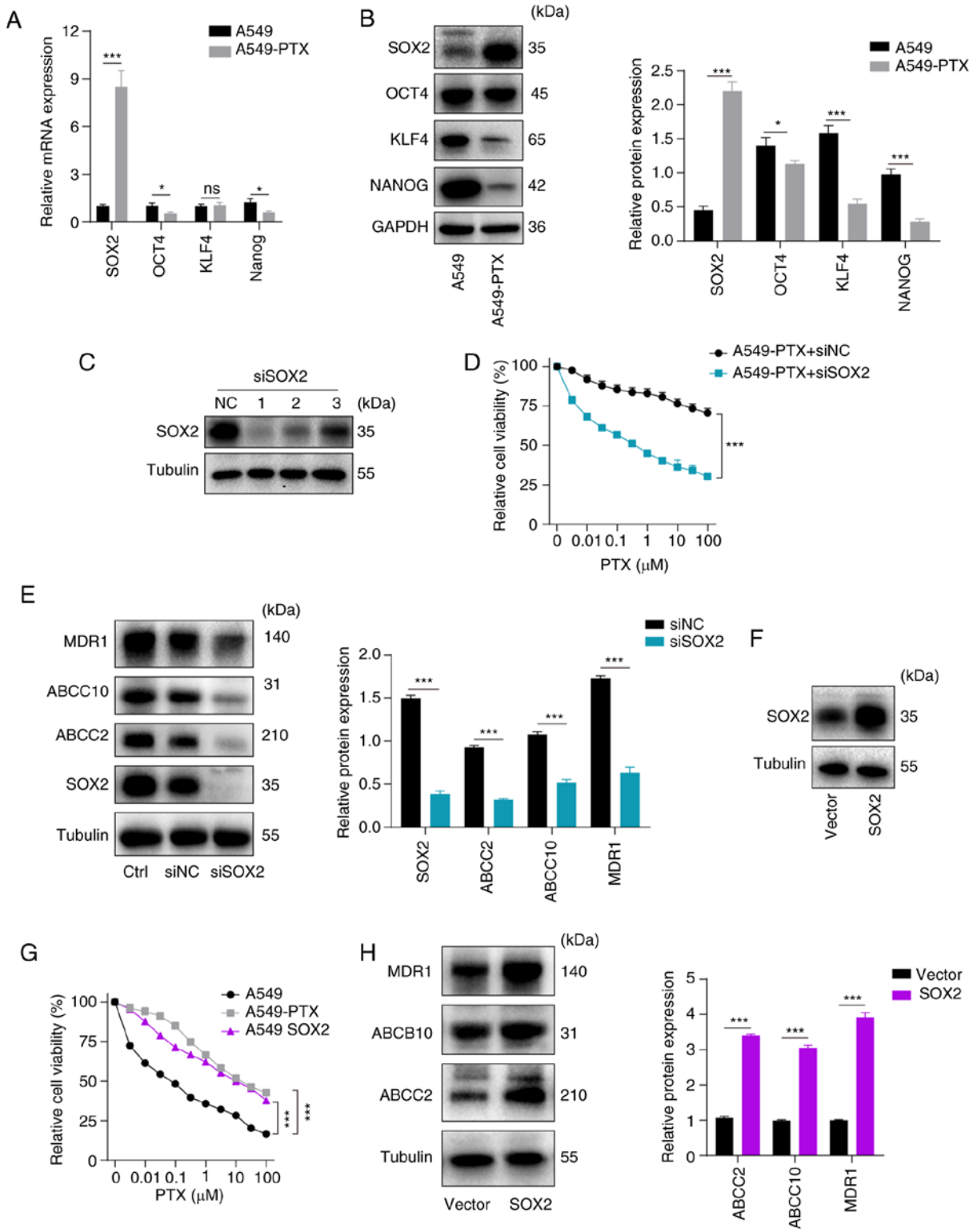

Figure 3. Higher levels of SOX2 confer PTX resistance in A549 non-small cell lung cancer cells. (A) mRNA expression levels of stemness-related genes were measured by reverse transcription-quantitative PCR in A549 and A549-PTX cells. (B) (Left) Protein expression levels of NANOG, KLF4, OCT4 and SOX2 were examined by western blotting in A549 and A549-PTX cells. (Right) Protein expression was semi-quantified using ImageJ. (C) Protein expression levels of SOX2 were examined by western blotting in A549-PTX cells transfected with siNC or SOX2 siRNA (siSOX2-1, siSOX2-2 and siSOX2-3). (D) Viability was examined using CCK-8 assays in A549-PTX cells transfected with siSOX2 or its control and treated with PTX for 48 h. (E) (Left) Protein expression levels of MDR1, ABCC10, ABCC2 and SOX2 were examined by western blotting in A549-PTX cells transfected with siSOX2 or its control. (Right) Protein expression was semi-quantified using ImageJ. (F) Protein expression levels of SOX2 were examined by western blotting in A549 cells overexpressing SOX2 or its vector control. (G) Viability was examined using CCK-8 assays in A549, A549-PTX and SOX2-overexpressing A549 cells treated with PTX for 48 h. (H) (Left) Protein expression levels of MDR1, ABCC10 and ABCC2 were examined by western blotting in A549 cells overexpressing SOX2 or its vector control. (Right) Protein expression was semi-quantified using ImageJ. GAPDH or Tubulin were used as a loading control in western blotting. All data are presented as the mean ± standard deviation. *P<0.05, ***P<0.001. ns, not significant. Relative, vs. respective control. SOX2, SRY-box transcription factor 2; PTX, paclitaxel; A549-PTX cells, PTX-resistant A549 non-small cell lung cancer cells; KLF4, Krüppel like factor 4; OCT4, octamer-binding transcription factor 4; siRNA/si, small interfering RNA; siNC, control siRNA; CCK-8, Cell Counting Kit-8; MDR1, multidrug resistance mutation 1; ABCC10, ATP binding cassette subfamily C member 10; ABCC2, ATP binding cassette subfamily C member 2; Ctl, control.

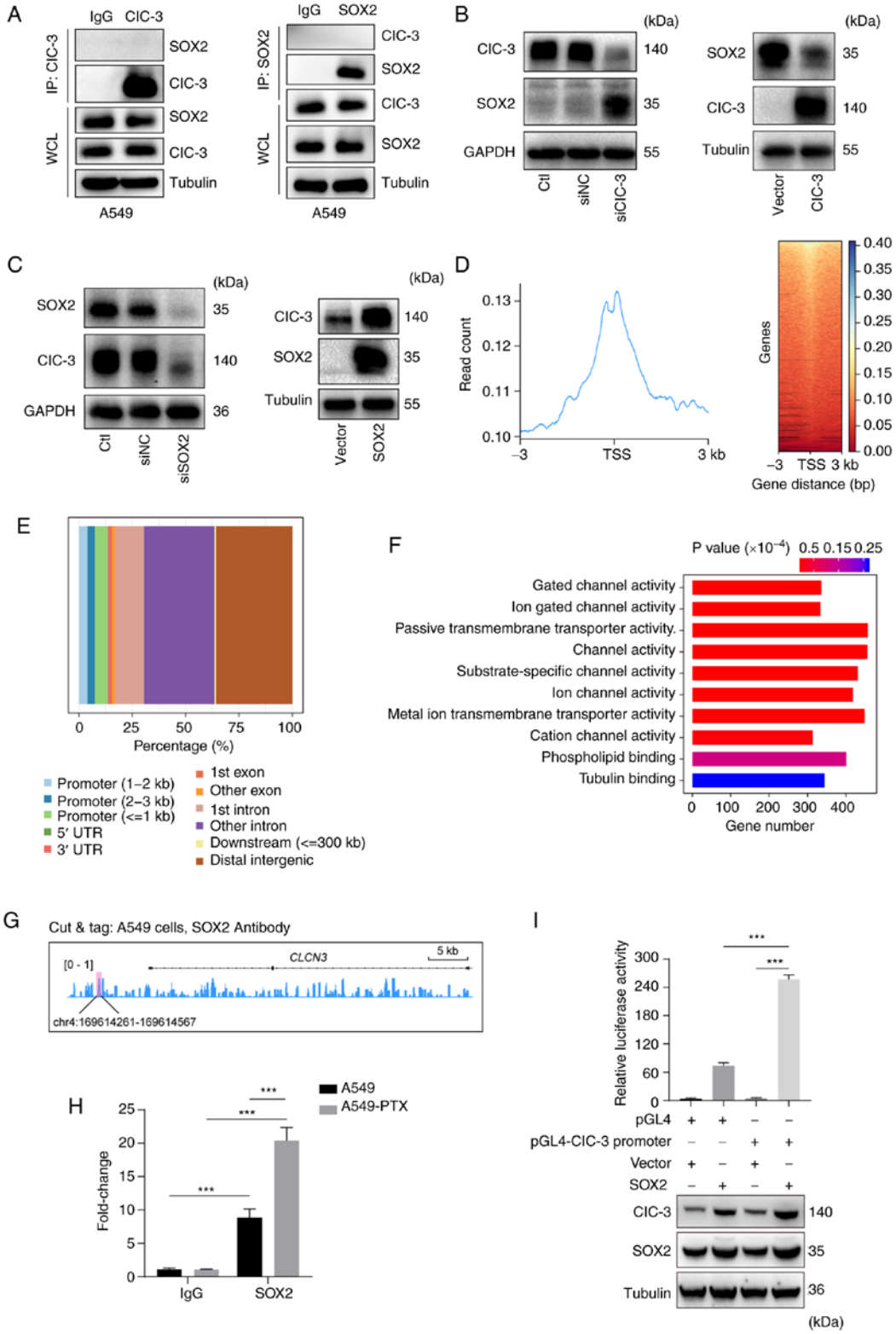

Figure 4. SOX2 promotes ClC-3 expression. (A) (Left) ClC-3 antibody or (right) SOX2 antibody was used to immunoprecipitate SOX2 or ClC-3 in A549 cells. IgG was used as the negative control. (B) Protein expression levels of ClC-3 and SOX2 in A549 cells transfected with (left) siClC-3 or (right) ClC-3 overexpression vector were examined by western blotting. (C) Protein expression levels of ClC-3 and SOX2 in A549 cells transfected with (left) siSOX2 or (right) SOX2 overexpression vector were examined by western blotting. (D) (Left) SOX2 binding peaks within 3 kb of the gene TSS determined by CUT&Tag analysis of A549 cells. (Right) Binding density of SOX2 was visualized using deepTools. The heatmap presents the CUT&Tag tag counts on the different SOX2 binding peaks in A549 cells. (E) Genome-wide distribution of SOX2-binding peaks in A549 cells. (F) Gene Ontology analysis of the SOX2-binding peaks at candidate target genes. (G) Genome browser tracks of CUT&Tag signal at the ClC-3 loci. The red area is the predicted SOX2 binding site in the promoter of *CLCN3*. (H) Changes of ClC-3-binding levels in A549 cells were determined by reverse transcription-quantitative PCR and presented as relative fold-change to the control after normalization as described in the materials and methods section. (I) (Above) Luciferase assay in A549 cells after co-transfection with the indicated plasmids. (Below) Protein expression levels of ClC-3 and SOX2 in A549 cells co-transfected with the indicated plasmids. GAPDH or tubulin were used as a loading control in western blotting. All data are presented as the mean ± standard deviation. ***P<0.001. Relative, vs. respective control. SOX2, SRY-box transcription factor 2; ClC-3, chloride voltage-gated channel 3; A549-PTX cells, paclitaxel-resistant A549 non-small cell lung cancer cells; siRNA/si, small interfering RNA; siNC, control siRNA; TSS, transcription start sites; CUT&Tag, cleavage under targets and tagmentation; IP, immunoprecipitation.

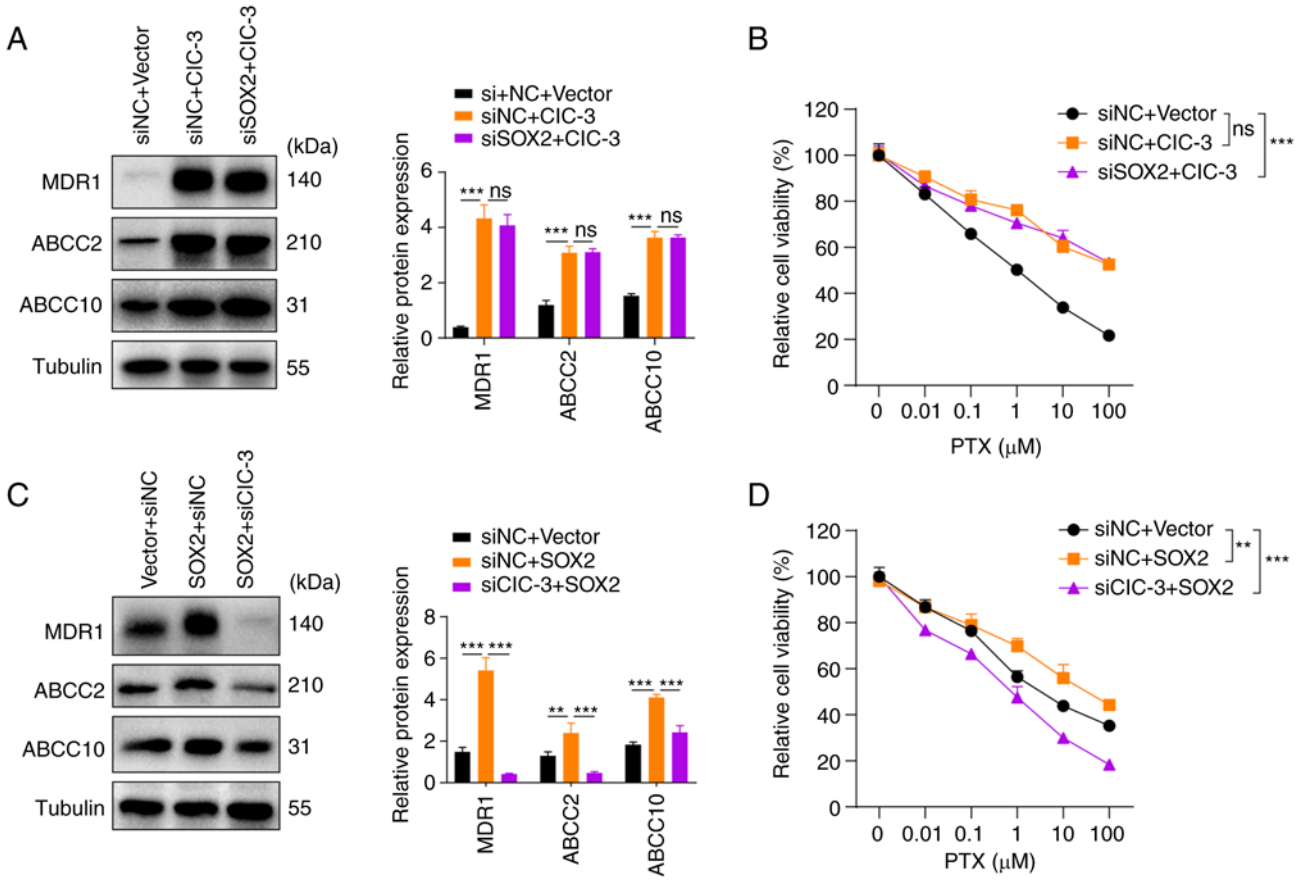

Figure 5. Knockdown of ClC-3 expression in A549 cells prevents PTX resistance induced by upregulation of SOX2 expression. (A) (Left) Protein expression levels of MDR1, ABCC2, ABCC10 and tubulin in A549 cells transfected with ClC-3 plasmid or siSOX2 and its control vector or siNC. (Right) Protein expression was semi-quantified using ImageJ. (B) Viability was examined using a CCK-8 assay in A549 cells transfected with ClC-3 plasmid or siSOX2 and its control vector or siNC. Cells were treated with PTX for 48 h. (C) (Left) Protein expression levels of MDR1, ABCC2, ABCC10 and tubulin in A549 cells transfected with SOX2 plasmid or siClC-3 and its control vector or siNC. (Right) Protein expression was semi-quantified using ImageJ. (D) Viability was examined using a CCK-8 assay in A549 cells transfected with SOX2 plasmid or siClC-3 and its control vector or siNC. Cells were treated with PTX for 48 h. Tubulin were used as a loading control in western blotting. All data are presented as the mean ± standard deviation. **P<0.005, ***P<0.001. ns, not significant. Relative, vs. respective control. ClC-3, chloride voltage-gated channel 3; A549-PTX cells, paclitaxel-resistant A549 non-small cell lung cancer cells; PTX, paclitaxel; MDR1, multidrug resistance mutation 1; ABCC2, ATP binding cassette subfamily C member 2; ABCC10, ATP binding cassette subfamily C member 10; siRNA/si, small interfering RNA; CCK-8, Cell Counting Kit-8.

the attendant epigenetic modulatory impacts of SOX2 in A549 cells, the target genes of different SOX2 binding peaks at the promoter were classified into different GO pathways. These GO pathways included 'Gated channel activity', 'Ion gated channel activity', 'Passive transmembrane transporter activity', 'Channel activity' and 'Cation channel activity' (Fig. 4F). Specifically, the binding of SOX2 on ClC-3 (*ClCN3*) loci is shown in Fig. 4G and the potential SOX2 binding site in the promoter of *ClCN3* was in chr4:169614261-169614567. CUT&Tag-qPCR analysis indicated that the SOX2 levels on ClC-3 promoters were significantly elevated in A549-PTX cells compared with A549 cells (Fig. 4H). A dual-luciferase reporter gene assay revealed that the luciferase activity in cells infected with the SOX2 vector was increased compared with that in cells infected with the promoter vector (Fig. 4I). These results suggested that SOX2 could promote gene transcription of ClC-3.

SOX2 promotes PTX resistance of A549 cells via ClC-3 expression. The aforementioned results indicated that SOX2 promoted the transcriptional expression of ClC-3 in PTX-resistant A549 NSCLC cells. The present study subsequently explored whether SOX2 mediates PTX resistance via ClC-3 expression. Western blotting and cell viability assay results revealed that silencing of SOX2 could not reverse the PTX resistance induced by ClC-3 overexpression (Fig. 5A and B); however, knockdown of ClC-3 expression in A549 cells prevented PTX resistance induced by upregulation of SOX2 expression (Fig. 5C and D). Collectively, these results provided additional evidence suggesting that SOX2 modulates PTX resistance via ClC-3.

Discussion

NSCLC is the main type of lung cancer with a high incidence and mortality (2). PTX is a broad-spectrum anticancer drug; however, development of resistance to PTX remains an important clinical problem (32,33). Previous research has demonstrated that CSCs have the ability of self-renewal and multi-directional differentiation, which is related to tumor progression, metastasis, drug resistance and tumor recurrence (34). CSCs are considered to be the main cause of

chemotherapy resistance and tumor recurrence (21,22). SOX2 is a key transcription factor maintaining the pluripotency of stem cells and serves a key role in maintaining stemness and conferring chemotherapy resistance. Piva *et al* (35) revealed that the tamoxifen resistance of breast cancer cells is related to SOX2-dependent activation of Wnt signaling. MLN4924 inhibits stem cell properties and makes cancer cells sensitive to chemotherapy by inactivating the F-box and WD repeat domain containing 2/msh homeobox 2/SOX2 axis in human lung cancer (36). Silencing of SOX2 increases the sensitivity to cisplatin in NSCLC by regulating apurinic/apyrimidinic endonuclease 1 signaling (26). The present study revealed that the mRNA and protein expression levels of SOX2 were increased in A549-PTX cells. SOX2 silencing in A549-PTX cells decreased viability by increasing the sensitivity to PTX; however, overexpression of SOX2 reversed these effects.

Chloride channels serve an important role in tumor drug resistance and have attracted wide attention. For example, ClC-3 increases the proportion of the free form of β-tubulin and decreases the proportion of the polymerized form of β-tubulin and finally decreases ovarian cancer cell sensitivity to PTX by interacting with SOX2 (16). ClC-3 participates in PTX resistance in A549 lung cancer cells through NF-κB signaling-dependent P-gp expression (17). Chloride voltage-gated channel 5 (ClC-5) induces multiple myeloma cell drug resistance to bortezomib by increasing pro-survival autophagy by inhibiting the AKT-mTOR signaling pathway (37). In the present study, PTX-resistant A549 cells were established according to a previous protocol (27). The protein and mRNA expression levels of drug resistance-related genes were increased in A549-PTX cells. ClC-3 was upregulated in A549-PTX cells. Treatment with DIDS, a chloride channel inhibitor, increased the sensitivity to PTX and downregulation of ClC-3 expression in PTX-resistant A549 NSCLC cells could significantly increase the sensitivity to PTX. However, the relationship between SOX2 and ClC-3 in PTX-resistant NSCLC cells is unclear.

Our previous study showed that SOX2 regulates the progression of prostate cancer cells by interacting with ClC-3 (30); however, there was no interaction between SOX2 and ClC-3 in PTX-resistant A549 NSCLC cells. Furthermore, ClC-3 is a downstream molecule of SOX2; however, SOX2 expression was increased following transfection with siClC-3 and SOX2 expression was decreased by ClC-3 overexpression. It has been previously reported that microRNA (miR)-103 increases PC-12 cell viability and reduced cell apoptosis via upregulation of SOX2 (38). Low miR-1181 expression increases pancreatic cancer cell viability and reduces cell apoptosis via upregulation of SOX2 and STAT3 (39). PTX has been reported to induce cell apoptosis in various tumors (40). It was hypothesized that SOX2 may protect against apoptosis and SOX2 expression was upregulated after transfection with siClC-3. Additionally, SOX2 combined with the promoter of ClC-3 and increased the transcriptional activity of ClC-3 in PTX-resistant A549 NSCLC cells. Recent studies have indicated that SOX2 combined with β-catenin and increased the transcriptional activity of ABCC2 to promote chemoresistance in colorectal cancer (41,42). Furthermore, SOX2 cooperates with Nup153 to control transcriptional programs in neural progenitor cells (NeuPCs) to enable bimodal gene regulation and maintenance of NeuPCs (43). Therefore, it was hypothesized that the transcriptional regulation of ClC-3 by SOX2 is an indirect regulation. SOX2 may interact with other factors to regulate the transcription of ClC-3. The factors which combine with SOX2 warrant further exploration.

Researchers have found that a variety of ion channels, such as voltage-gated K^+, Na^+, Ca^{2+} and transient receptor potential channels, as well as epithelial Na^+/degenerin family ion channels except chloride channels, are abnormally expressed in various cancer types and are involved in the growth, migration, invasion and drug resistance of cancer cells (44-46). Notably, GO enrichment of CUT&Tag analysis showed that SOX2 also regulated the transcription of other ion channel genes, including 'Gated channel activity', 'Ion gated channel activity', 'Passive transmembrane transporter activity', 'Channel activity' and 'Cation channel activity'.

Weinstein (47) indicated that gene addiction is a potential Achilles' heel of cancer, that is, the expression of oncogenes is necessary not only to initiate tumorigenesis, but also to maintain malignant phenotypes, such as tumor invasion, metastasis and drug resistance (48-49). In order to survive, tumor cells would promote the emergence of new tumor clones or develop gene mutations that make tumors insensitivity to drug treatment (50). For example, targeting BCR-ABL fusion gene with the small molecule inhibitor serine/threonine kinase inhibitor Gleevec could cure chronic myelogenous leukemia patients. However, despite the great clinical success of Gleevec, the drug resistance of Gleevec has also developed, which is caused by obtaining mutations in the Gleevec binding site (51). It is evident that combined therapies are required to cure cancer. Given the important role of SOX2/ClC-3 axis in CSCs and PTX-resistance in NSCLC, it is hypothesized that SOX2/ClC-3-based therapy combined with PTX may be a promising path to pursue.

The current study only confirmed these results in A549 cells. NSCLC is a group of lung cancers with several subtypes such as squamous cell carcinoma, adenocarcinoma and large cell carcinoma (52). Other PTX NSCLC cells such H1299, PC9 and SPC-A1 will be generated to explore the consistency of SOX2/ClC-3 involved PTX resistance in different subtypes NSCLS cells. In addition, whether SOX2/ClC-3 axis is involved in PTX or other drug resistance in human lung cancer specimens will also be explored in future studies. In summary, the present study revealed a novel mechanism whereby the SOX2/ClC-3 axis regulates NSCLC PTX resistance. The present findings may contribute to the development of novel therapeutic candidates for NSCLC PTX resistance and provides potentially useful experimental evidence for PTX-resistant cancer therapy.

Acknowledgements

Not applicable.

Funding

The present study was supported by the Pearl River S&T Nova Program of Guangzhou (grant no. 201906010069 to HZ).

Availability of data and materials

The datasets used and/or analyzed during the present study are available from the corresponding author on reasonable request.

Authors' contributions

YH designed the study, analyzed the data and wrote the manuscript. XW and RH performed the study and data analysis. GP analyzed the data and constructed the graphs. XL wrote the manuscript and revised the manuscript. YH, XW and RH confirm the authenticity of all the raw data. All authors read and approved the final version of the manuscript.

Ethics approval and consent to participate

Not applicable.

Patient consent for publication

Not applicable.

Competing interests

The authors declare that they have no competing interests.

References

1. Sung H, Ferlay J, Siegel RL, Laversanne M, Soerjomataram I, Jemal A and Bray F: Global cancer statistics 2020: GLOBOCAN estimates of incidence and mortality worldwide for 36 cancers in 185 countries. CA Cancer J Clin 71: 209-249, 2021.
2. Herbst RS, Morgensztern D and Boshoff C: The biology and management of non-small cell lung cancer. Nature 553: 446-454, 2018.
3. Gildea TR, DaCosta Byfield S, Hogarth DK, Wilson DS and Quinn CC: A retrospective analysis of delays in the diagnosis of lung cancer and associated costs. Clinicoecon Outcomes Res 9: 261-269, 2017.
4. Travis WD: Lung cancer pathology: Current concepts. Clin Chest Med 41: 67-85, 2020.
5. Travis WD, Brambilla E, Nicholson AG, Yatabe Y, Austin JHM, Beasley MB, Chirieac LR, Dacic S, Duhig E, Flieder DB, *et al*: The 2015 World Health Organization classification of lung tumors: Impact of genetic, clinical and radiologic advances since the 2004 classification. J Thorac Oncol 10: 1243-1260, 2015.
6. Latimer KM: Lung cancer: Clinical presentation and diagnosis. FP Essent 464: 23-26, 2018.
7. Huang LT, Cao R, Wang YR, Sun L, Zhang XY, Guo YJ, Zhao JZ, Zhang SL, Jing W, Song J, *et al*: Clinical option of pemetrexed-based versus paclitaxel-based first-line chemotherapeutic regimens in combination with bevacizumab for advanced non-squamous non-small-cell lung cancer and optimal maintenance therapy: Evidence from a meta-analysis of randomized control trials. BMC Cancer 21: 426, 2021.
8. Jordan MA and Wilson L: Microtubules as a target for anticancer drugs. Nat Rev Cancer 4: 253-265, 2004.
9. Schiff PB, Fant J and Horwitz SB: Promotion of microtubule assembly in vitro by taxol. Nature 277: 665-667, 1979.
10. Weaver BA: How taxol/paclitaxel kills cancer cells. Mol Biol Cell 25: 2677-2681, 2014.
11. Cui H, Arnst K, Miller DD and Li W: Recent advances in elucidating paclitaxel resistance mechanisms in non-small cell lung cancer and strategies to overcome drug resistance. Curr Med Chem 27: 6573-6595, 2020.
12. Hong S, Bi M, Wang L, Kang Z, Ling L and Zhao C: CLC-3 channels in cancer (review). Oncol Rep 33: 507-514, 2015.
13. Mu H, Mu L and Gao J: Suppression of CLC-3 reduces the proliferation, invasion and migration of colorectal cancer through Wnt/β-catenin signaling pathway. Biochem Biophys Res Commun 533: 1240-1246, 2020.
14. Du S and Yang L: ClC-3 chloride channel modulates the proliferation and migration of osteosarcoma cells via AKT/GSK3β signaling pathway. Int J Clin Exp Pathol 8: 1622-1630, 2015.
15. Ye D, Luo H, Lai Z, Zou L, Zhu L, Mao J, Jacob T, Ye W, Wang L and Chen L: ClC-3 chloride channel proteins regulate the cell cycle by up-regulating cyclin D1-CDK4/6 through suppressing p21/p27 expression in nasopharyngeal carcinoma cells. Sci Rep 6: 30276, 2016.
16. Feng J, Peng Z, Gao L, Yang X, Sun Z, Hou X, Li E, Zhu L and Yang H: ClC-3 promotes paclitaxel resistance via modulating tubulins polymerization in ovarian cancer cells. Biomed Pharmacother 138: 111407, 2021.
17. Chen Q, Liu X, Luo Z, Wang S, Lin J, Xie Z, Li M, Li C, Cao H, Huang Q, *et al*: Chloride channel-3 mediates multidrug resistance of cancer by upregulating P-glycoprotein expression. J Cell Physiol 234: 6611-6623, 2019.
18. Weylandt KH, Nebrig M, Jansen-Rosseck N, Amey JS, Carmena D, Wiedenmann B, Higgins CF and Sardini A: ClC-3 expression enhances etoposide resistance by increasing acidification of the late endocytic compartment. Mol Cancer Ther 6: 979-986, 2007.
19. Han Y, Zhou Y, Zhou L, Jia X, Yu X, An X and Shi Z: Blockade of chloride channel-3 enhances cisplatin sensitivity of cholangiocarcinoma cells though inhibiting autophagy. Can J Physiol Pharmacol 100: 584-593, 2022.
20. Ajani JA, Song S, Hochster HS and Steinberg IB: Cancer stem cells: The promise and the potential. Semin Oncol 42 (Suppl 1): S3-S17, 2015.
21. Donnenberg VS and Donnenberg AD: Multiple drug resistance in cancer revisited: The cancer stem cell hypothesis. J Clin Pharmacol 45: 872-877, 2005.
22. Phi LTH, Sari IN, Yang YG, Lee SH, Jun N, Kim KS, Lee YK and Kwon HY: Cancer stem cells (CSCs) in drug resistance and their therapeutic implications in cancer treatment. Stem Cells Int 2018: 5416923, 2018.
23. Zhou C, Yang X, Sun Y, Yu H, Zhang Y and Jin Y: Comprehensive profiling reveals mechanisms of SOX2-mediated cell fate specification in human ESCs and NPCs. Cell Res 26: 171-189, 2016.
24. Liu K, Lin B, Zhao M, Yang X, Chen M, Gao A, Liu F, Que J and Lan X: The multiple roles for Sox2 in stem cell maintenance and tumorigenesis. Cell Signal 25: 1264-1271, 2013.
25. Song WS, Yang YP, Huang CS, Lu KH, Liu WH, Wu WW, Lee YY, Lo WL, Lee SD, Chen YW, *et al*: Sox2, a stemness gene, regulates tumor-initiating and drug-resistant properties in CD133-positive glioblastoma stem cells. J Chin Med Assoc 79: 538-545, 2016.
26. Chen TY, Zhou J, Li PC, Tang CH, Xu K, Li T and Ren T: SOX2 knockdown with siRNA reverses cisplatin resistance in NSCLC by regulating APE1 signaling. Med Oncol 39: 36, 2022.
27. Huang C, Zhang X, Jiang L, Zhang L, Xiang M and Ren H: FoxM1 induced paclitaxel resistance via activation of the FoxM1/PHB1/RAF-MEK-ERK pathway and enhancement of the ABCA2 transporter. Mol Ther Oncolytics 14: 196-212, 2019.
28. Livak KJ and Schmittgen TD: Analysis of relative gene expression data using real-time quantitative PCR and the 2(-Delta Delta C(T)) method. Methods 25: 402-408, 2001.
29. Prieto-Vila M, Takahashi RU, Usuba W, Kohama I and Ochiya T: Drug resistance driven by cancer stem cells and their niche. Int J Mol Sci 18: 2574, 2017.
30. Chen J, Wang F, Lu Y, Yang S, Chen X, Huang Y and Lin X: CLC-3 and SOX2 regulate the cell cycle in DU145 cells. Oncol Lett 20: 372, 2020.
31. Wu Q, Zhang L, Su P, Lei X, Liu X, Wang H, Lu L, Bai Y, Xiong T, Li D, *et al*: MSX2 mediates entry of human pluripotent stem cells into mesendoderm by simultaneously suppressing SOX2 and activating NODAL signaling. Cell Res 25: 1314-1332, 2015.
32. Adrianzen Herrera D, Ashai N, Perez-Soler R and Cheng H: Nanoparticle albumin bound-paclitaxel for treatment of advanced non-small cell lung cancer: An evaluation of the clinical evidence. Expert Opin Pharmacother 20: 95-102, 2019.
33. Scripture CD, Figg WD and Sparreboom A: Paclitaxel chemotherapy: From empiricism to a mechanism-based formulation strategy. Ther Clin Risk Manag 1: 107-114, 2005.
34. Sullivan JP, Minna JD and Shay JW: Evidence for self-renewing lung cancer stem cells and their implications in tumor initiation, progression, and targeted therapy. Cancer Metastasis Rev 29: 61-72, 2010.

35. Piva M, Domenici G, Iriondo O, Rábano M, Simões BM, Comaills V, Barredo I, López-Ruiz JA, Zabalza I, Kypta R and Vivanco MD: Sox2 promotes tamoxifen resistance in breast cancer cells. EMBO Mol Med 6: 66-79, 2014.
36. Yin Y, Xie CM, Li H, Tan M, Chen G, Schiff R, Xiong X and Sun Y: The FBXW2-MSX2-SOX2 axis regulates stem cell property and drug resistance of cancer cells. Proc Natl Acad Sci USA 116: 20528-20538, 2019.
37. Zhang H, Pang Y, Ma C, Li J, Wang H and Shao Z: ClC5 decreases the sensitivity of multiple myeloma cells to bortezomib via promoting prosurvival autophagy. Oncol Res 26: 421-429, 2018.
38. Li G, Chen T, Zhu Y, Xiao X, Bu J and Huang Z: MiR-103 alleviates autophagy and apoptosis by regulating SOX2 in LPS-injured PC12 cells and SCI rats. Iran J Basic Med Sci 21: 292-300, 2018.
39. Jiang J, Li Z, Yu C, Chen M, Tian S and Sun C: MiR-1181 inhibits stem cell-like phenotypes and suppresses SOX2 and STAT3 in human pancreatic cancer. Cancer Lett 356: 962-970, 2015.
40. Khing TM, Choi WS, Kim DM, Po WW, Thein W, Shin CY and Sohn UD: The effect of paclitaxel on apoptosis, autophagy and mitotic catastrophe in AGS cells. Sci Rep 11: 23490, 2021.
41. Zhu Y, Huang S, Chen S, Chen J, Wang Z, Wang Y and Zheng H: SOX2 promotes chemoresistance, cancer stem cells properties, and epithelial-mesenchymal transition by β-catenin and Beclin1/autophagy signaling in colorectal cancer. Cell Death Dis 12: 449, 2021.
42. Kim BH, Oh HK, Kim DW, Kang SB, Choi Y and Shin E: Clinical implications of cancer stem cell markers and ABC transporters as a predictor of prognosis in colorectal cancer patients. Anticancer Res 40: 4481-4489, 2020.
43. Toda T, Hsu JY, Linker SB, Hu L, Schafer ST, Mertens J, Jacinto FV, Hetzer MW and Gage FH: Nup153 interacts with Sox2 to enable bimodal gene regulation and maintenance of neural progenitor cells. Cell Stem Cell 21: 618-634.e7, 2017.
44. Wulff H, Castle NA and Pardo LA: Voltage-gated potassium channels as therapeutic targets. Nat Rev Drug Discov 8: 982-1001, 2009.
45. Yamashita N, Hamada H, Tsuruo T and Ogata E: Enhancement of voltage-gated Na+ channel current associated with multidrug resistance in human leukemia cells. Cancer Res 47: 3736-3741, 1987.
46. Catterall WA and Swanson TM: Structural basis for pharmacology of voltage-gated sodium and calcium channels. Mol Pharmacol 88: 141-150, 2015.
47. Weinstein IB: Cancer. Addiction to oncogenes-the Achilles heal of cancer. Science 297: 63-64, 2002.
48. Yan W, Zhang W and Jiang T: Oncogene addiction in gliomas: Implications for molecular targeted therapy. J Exp Clin Cancer Res 30: 58, 2011.
49. Nagel R, Semenova EA and Berns A: Drugging the addict: Non-oncogene addiction as a target for cancer therapy. EMBO Rep 17: 1516-1531, 2016.
50. Sosa Iglesias V, Giuranno L, Dubois LJ, Theys J and Vooijs M: Drug resistance in non-small cell lung cancer: A potential for NOTCH targeting? Front Oncol 8: 267, 2018.
51. Gorre ME, Mohammed M, Ellwood K, Hsu N, Paquette R, Rao PN and Sawyers CL: Clinical resistance to STI-571 cancer therapy caused by BCR-ABL gene mutation or amplification. Science 293: 876-880, 2001.
52. Pikor LA, Ramnarine VR, Lam S and Lam WL: Genetic alterations defining NSCLC subtypes and their therapeutic implications. Lung Cancer 82: 179-189, 2013.